A new design of electro-optical modulator with domain-inverted technology

YiYun Wang, XianFeng Chen, QingJi Zeng, YuXing Xia
Center of Broad-band Optical Networking Technology, Shanghai JiaoTong University,
Rm 1708 HaoRan Building., 1954 HuaShan Rd., ShangHai, China

Abstract:
Our interests focus on the new theme of electro-optical modulator relevant to the development of domain-inverted $LiNbO_3$ waveguide technology. By means of the theory of dielectric planar optical waveguide, we have not only computed and drew the corresponding characteristic figures of domain-inverted $LiNbO_3$ waveguide electro-optical modulator with variable parameters, but also given the explanation of linear area involving input and output ports in theory. In addition, some improving and revising thoughts about buffer layer and electrooptic efficiency of such modulator is done. We have experimented a lot mainly including steps of the domain-inverse poling techniques to validate the feasibility of making the smart structure of modulator.

Keywords:
Lithium Niobate, Mach-Zehnder interferometer, Quasi-Phase Matched, Pyroelectric, Voltage-induced, Planar waveguide, Chirp-free

I. Introduction

Among these devices for optical communication, optical signal modulators have taken up importance all along in that such modulators are not only the major access to network for various information media, but also a common manner of processing the signal in the network. People have been doing comprehensive and profound research of optical modulators a long time for broad applications in variable network environment. According to the mechanism of modulating the electronic signal, electro-optical modulators could be classified with internal and external modulators. Typical internal modulator is designed by altering the parameters of laser to change optical amplitude or phase directly. Traditional external electro-optical modulators include all kinds of modulators constructed by special mediums such as compounds, crystals and polymers with excellent electro-optical characters. In higher speed digital communication applications, fiber dispersion has limited system performance. Lithium Niobate ($LiNbO_3$) external modulators provide both the required bandwidth and the equally important means for minimizing the effects of dispersion. Unlike direct modulation of a laser diode, $LiNbO_3$ guided-wave modulators can be designed for zero-chirp or adjustable-chirp operation which can help to minimize the system degradation associated with fiber dispersion. Moreover, in analog systems, linearized external modulators can provide very low modulation distortion.

The research of modulators made by Lithium Niobate have been carrying on for a few decades Lithium Niobate has a very high intrinsic modulation bandwidth and limited switching speeds because of a variety of physical constraints. Modulation is produced by a voltage-induced change in the refractive index. The achievable index change is relatively small and, thus, either large voltages or long electrode lengths are needed to obtain sufficient modulation. For higher bandwidths, the mismatch between the electrical and optical propagation constants as well as by the electrical attenuation of the electrode should also be considered and solved partly.

Traditional external Lithium Niobate modulator refer to Mach-Zehnder interferometer(MZI) modulator which can be several centimeters long, and have necessary parts including electrooptic substrate, electrode metal, electrode adhension layer, buffer layer and the dopant used for fabrication of the optical waveguides. The basic building blocks for $LiNbO_3$ modulators generally fall into two categories --- MZI type or directional coupler type. The MZI works well with high-bandwidth electrode structures requiring tens of micrometers of spacing between waveguides, and long electrodes are needed to reduce drive voltages. The directional-coupler-type switches are typically used for lower speed switching applications where small size and polarization diversity may be required, and tight electrode gaps are more easily accommodated.

In this paper, we will present and analyze a new approach of making EO modulator with the technology of domain-inverted $LiNbO_3$ waveguide. By means of the theory of dielectric planar optical waveguide, we not only have computed and drew the corresponding characteristic figures of domain-inverted $LiNbO_3$ waveguide electro-optical modulator with variable parameters, e.g. input optical guided-wave mode, optical intensity and wavelength, but also give the explanation of linear area involving input and output ports in theory. In addition, some discussion about the response time and rate of modulation of such modulator is done.

II. Theoretical deduction

The dielectric planar optical waveguide is a kind of component propagating and constraining the way of light within optical waveguide devices and integrated optical circuits. Due to the simple geometric shape of planar waveguide, the fundamental mode and subsidiary modes could be depicted by apparent equations and its relevant characters will be solved with the aid of computer in theory. Although the structure of the new design of EO modulator is not so complex, its feasibility has not been verified to ensure a reasonable range or conditions for modulating the signal. So it is necessary to conduct a detailed theoretical computation for the new design before further planning.

Similar to the making technology of waveguide quasi-phase matched (QPM) nonlinear optic devices which can perform a variety of wavelength conversion functions, the new scheme needs the formation of Ferro-electric-domain-inverted gratings. However, we propagate the original light along a single channel within a period of grating and modulate the light through a thin electrode over the domain-inverted area. So multiple EO modulators could be integrated into a single $LiNbO_3$ wafer by careful adjustment of waveguide parameters easily achievable according to current domain-inverse poling techniques.

The first choice encountered in designing a $LiNbO_3$ modulator is the orientation of the crystal axes to the waveguides and electrodes. The crystal cut affects both modulator efficiency, as denoted by half-wave voltage V_π, and modulator chirp, which is described by the chirp parameter α. The strongest component of the applied electric field must be aligned with the z-axis of the crystal, which has the highest electrooptic coefficient. This requires that the waveguide be placed between the electrodes for an x-cut configuration and beneath the electrodes for z-cut. When the signal voltage is added along z-axis, the refractive index of raw $LiNbO_3$ wafer along z axis is

$$n_z = n_e - \frac{1}{2} \cdot n_e^3 \cdot r_{33} \cdot E \qquad (2\text{-}1)$$

Where E is applied electric field in z-direction, n_e is abnormal refractive index and the coefficient of r_{33} in $LiNbO_3$ is 30.8×10^{-12} m/v.

If we change the specific area as domain-inverted area, the above refractive index will be

$$n_z = n_e + \frac{1}{2} \cdot n_e^3 \cdot r_{33} \cdot E \qquad (2\text{-}2)$$

So the difference of refractive index is

$$\Delta n = n_e^3 \cdot r_{33} \cdot E = n_e^3 \cdot r_{33} \cdot \frac{U}{d} \qquad (2\text{-}3)$$

Calculated by assuming that the applied electric field is even and the side effect could be ignored.

The ability of constraining the light in waveguide is changed with varied applied voltage which causing the varied Δn. If the output power of light is linearly changed with applied signal voltage within a reasonable range and provides a little dispersion, the special area in $LiNbO_3$ wafer could make a voltage-induced amplitude modulator.

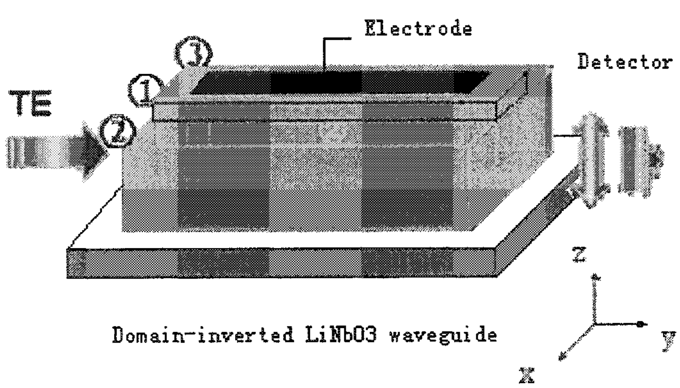

Fig.1 The schematic diagram of domain-inverted $LiNbO_3$ waveguide

Fig.1 depicts a three-dimensional view of an x-cut $LiNbO_3$ sample modulator. In order to keep the light to propagate in the middle film, the condition of maintaining the guided modes in planar waveguide is

$$kh - \phi_{13} - \phi_{12} = m\pi \qquad (2\text{-}4)$$

Where k is the value of wave vector along x-axis, h is the thickness of middle film and m is the number of mode. Replace ϕ_{12} and ϕ_{13} with their expression formulae and define the effective refractive index of waveguide $N=\frac{\beta}{k_0}=n_1\cdot\sin\theta$, so we can get the eigenvalue equations of guided mode for two basic different polarization beams.

For TE mode,

$$\sqrt{(n_1^2-N^2)}\cdot k_0\cdot h=m\pi+arctg\sqrt{\frac{N^2-n_2^2}{n_1^2-N^2}}+arctg\sqrt{\frac{N^2-n_3^2}{n_1^2-N^2}} \quad (2\text{-}5)$$

For TM mode,

$$\sqrt{(n_1^2-N^2)}\cdot k_0\cdot h=m\pi+arctg[(\frac{n_1^2}{n_2^2})\sqrt{\frac{N^2-n_2^2}{n_1^2-N^2}}]+arctg[\frac{n_1^2}{n_3^2}\cdot\sqrt{\frac{N^2-n_3^2}{n_1^2-N^2}}] \quad (2\text{-}6)$$

According to the analysis of symmetric and asymmetric planar waveguide, we know that the fundamental mode of symmetric planar waveguide could not be aborted while a cut-off condition for guided mode lies in asymmetric planar waveguide. So we define the normalized thickness V

$$V=\sqrt{n_1^2-n_2^2}\cdot k_0\cdot h \quad (2\text{-}7)$$

By solving the eigenvalue equation, we could find that the number of guided mode decreases with smaller value of V and the waveguide has not any guided modes in case that the film thickness h, optical frequency ω and $(n_1^2-n_2^2)$ are all small enough. When V=kh, there is at least one guided mode in the waveguide.

In order to manifest the fundamental character, assuming that the light of basic mode TE couple in the waveguide, we could get a set of formulae including the number of guided mode, and the transfer function between the applied voltage and the output power.

The guided mode equation:

$$V\cdot\sqrt{1-b_{TE}}=m\pi+2\cdot arctg(\sqrt{\frac{b_{TE}}{1-b_{TE}}}) \quad (2\text{-}8)$$

$$\text{Where } b_{TE}=\frac{\frac{1}{k_0^2}\cdot\beta^2-n_2^2}{n_1^2-n_2^2} \quad (2\text{-}9)$$

The output power vs. the applied voltage equation:

$$P=\frac{2wk^2+(k-\frac{q^2}{k})\cdot\sin(2kw)+2q[1+qw-\cos(2kw)]}{4n_e\cdot\Delta n\cdot(wk_0^2+\frac{2k_0}{\sqrt{N^2-n_2^2}})} \quad (2\text{-}10)$$

$$1+tg^2(\frac{k_0wr}{2})=\frac{2n_e\cdot\Delta n}{r^2} \quad (2\text{-}11)$$

Where k, q, N, Δn, n_e is decided by definition respectively.

There are typical figures drawn by computer according to the above analysis, which show the good linearism of the scheme in the range of 50v-200v.

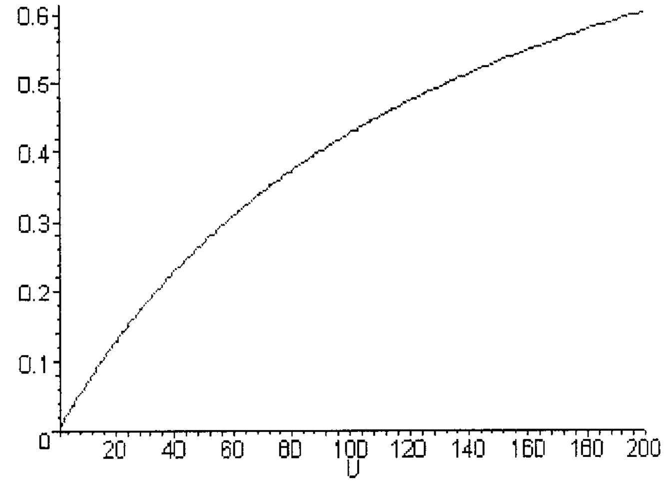

Fig 2. $\lambda = 0.6828$ μm, w =9 μm , d=300 μm (25 ℃)

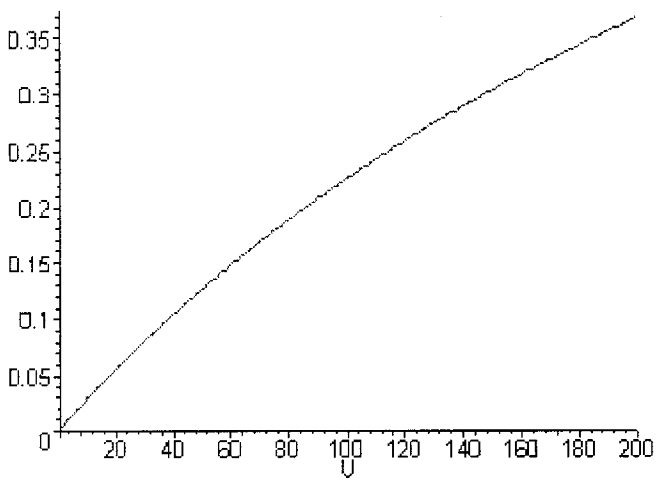

Fig 3. $\lambda = 1.064$ μm, w =9 μm, d=300 μm (25 ℃)

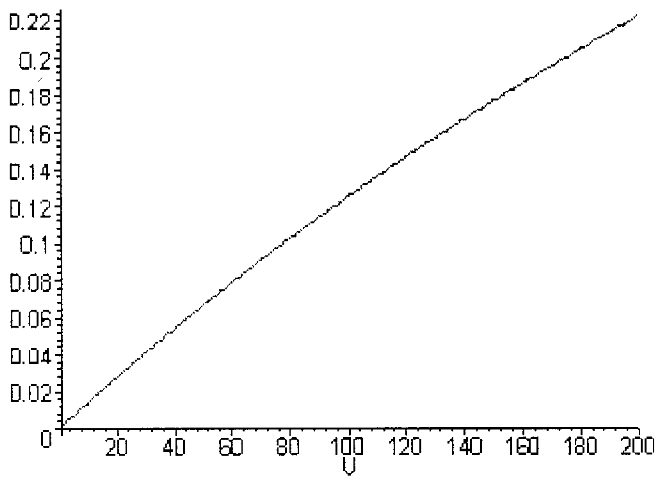

Fig 4. $\lambda = 1.5$ μm, w =9 μm, d=300 μm (25 ℃)

After the first validation of feasibility of the new idea, we have conducted a set of practical experiments including steps of the domain-inverse poling techniques, such as cleaning, coating, lithography, sputtering, poling, plating electrode and so on. In addition, some improving and revising thoughts are added in the design of a concrete EO modulator. There are mainly two aspects for further design. One is buffer layer, and another is the electrooptic efficiency.

III. Buffer layer & Electrooptic efficiency

Buffer layer

We experiment both structures with and without buffer layer. The results show that the waveguide should be placed between the electrodes for an x-cut configuration and beneath the electrodes for z-cut. Z-cut devices require a buffer layer to minimize attenuation of the optical mode due to metal absorption. Z-cut devices also employ conductive buffer layers and charge bleed layers to mitigate dc drift and pyroelectric charge buildup, respectively. Buffer layers are also required for broad-band velocity matching on both z-cut and x-cut devices due to the high dielectric constants of lithium niobate.

Electrooptic efficiency

The electrooptic efficiency of various electrode topologies and the applied electric field can be modeled using quasi-static techniques such as finite-element or finite-difference methods. X-cut electrode topologies result in chirp-free modulation due to the push-pull symmetry of the applied fields in the electrode gaps.

In z-cut devices, the waveguide positioned underneath the hot electrode experience a field flux that is more concentrated, resulting in a factor of two improvements in overlap between RF and optical field, relative to x-cut. The overall improvement in z-cut V_π is only about 20% for single-drive modulators which results in a chirp parameter of approximately -0.7. However, by employing a dual-drive topology, the factor of two improvements in overlap under the hot electrode can result in zero-chirp operation. In fact, a number of methods have been employed to enhance the electrooptic efficiency. The electrooptic efficiency at modulation frequency can be improved at the expense of bandwidth by using RF phase-matching techniques such as phase reversal or intermittent-interaction electrodes. The narrow-band techniques allow the buffer electrode structure to be optimized for the best field overlap.

The electrooptic efficiency versus modulation frequency is compared in Fig5,6 for the various electrode geometries and crystal cuts.

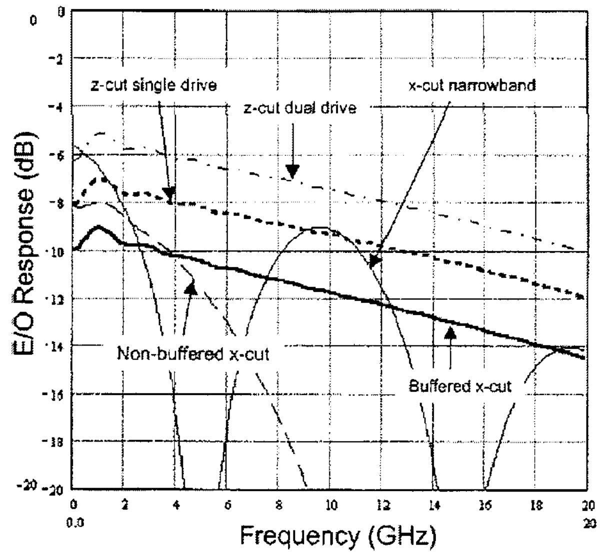

Fig5. Electrooptic response for broad-band digital or RZ pulsing applications at 2.5 or 10 Gb/s (no ridges or $\triangle$n enhancement).

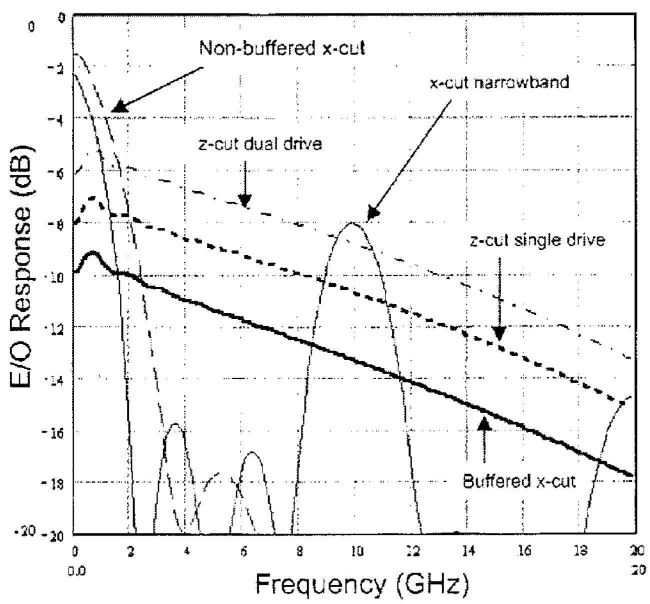

Fig6. Electrooptic response for the 5-cm electrode length (no ridges or $\triangle$n enhancement).

IV. Summary

$LiNbO_3$ modulators have found widespread use in fiber-optic communication systems, including both chirped and zero-chirp NRZ and RZ digital transmission formats. At the same time, device-manufacturing technology has progressed to enable extensive deployment within digital and analog communication systems. In this paper, we focus on the new theme of this research with the special domain-inverted technology. In spite of the whole production of modulator has not been completed, we have grasped the importance and the key making method by detailed theoretical deduction and practical experiments, especially in the modulating part, which enhance our interest firmly on such new method.

V. References

【1】 F. Heismann, S. K. Korotky, and J. J. Veselka, "Lithium niobate integrated optics: Selected contemporary devices and system applications," in Optical Fiber Telecommunications III B, I. P. Kaminow and T. L.Koch, Eds. New York: Academic, 1997, pp. 377–462.;

【2】 S.-J. Chang, C.-L. Tsai, Y.-B. Lin, J.-F. Liu, and W.-S. Wang, "Improved electro-optic modulator with ridge structure in x-cut LiNbO3 ," J. Light-wave Technol., vol. 17, pp. 843–847, 1999;

【3】 K. Noguchi, O. Mitomi, and H. Miyazawa, "Millimeter-wave Ti : LiNbO3 optical modulators," J. Lightwave Technol., vol. 16, pp.615–619, 1998.

【4】 P. Hallemeier, K. Kissa, G. McBrien, and T. Horton , "Next generation 10Gb/s lithium niobate modulator components for RZ based transmission techniques," in Proc. National Fiberoptic Engineers Conf., Sept.1999.

【5】 G. Gopalakrishnan, W. K. Burns, R. W. McElhanon, C. H. Bulmer, and A. S. Greenblatt, "Performance and modeling of broadband LiNbO3 traveling wave optical intensity modulators," J. Lightwave Technol., vol.12, pp. 1807–1819, 1994.

【6】 D. Maack , "Reliability of lithium niobate Mach-Zehnder modulators for digital optical fiber telecommunication systems," in Proc. SPIE Critical Reviews: Reliability of Optical Fibers and Optical Fiber Systems, Boston, MA, Sept. 1999, pp. 197–230.

【7】 W. L. Chen, R. S. Chen, J. H. Lee, and W. S. Wang, "Lithium Niobate ridge waveguides by nickel diffusion and proton-exchanged wet etching," IEEE Photon. Technol. Lett., vol. 7, pp. 1318–1320, 1995.

【8】 R. S. Moyer, R. Grencavich, F. F. Judd, R. C. Kershner, W. J. Minford, and R. W. Smith, "Design and qualification of hermetically packaged lithium niobate optical modulator," IEEE Trans. Comp., Packag., Manufact. Technol. B, vol. 21, pp. 130– 135, 1998.